JOURNAL OF SCIENCE TECHNOLOGY AND EDUCATION 14(1), JANUARY, 2026
E-ISSN: 3093-0898, PRINT ISSN: 2277-0011; Journal homepage: www.atbufstejoste.com

Development of a Radio Frequency Energy Harvesting System to Power Small Electronic Devices

Amanya Denis, Aliyu Hassan, Cartland Richard
Department of Electrical Engineering,
Faculty of Engineering, Technology, Applied Design and Fine Art,
Kabale University, Kabale, Uganda

ABSTRACT
Autonomous electronic loads such as remote sensors, IoT modules, and hidden micro-devices lack convenient or continuous access to traditional power lines. This can be addressed by harvesting ambient radio-frequency energy. The project designed and constructed a prototype system comprising a ferrite-rod and long-wire monopole antenna tuned via a gang-capacitor network, a Schottky-diode half-wave rectifier, and supercapacitor energy storage. Under optimal tuning at approximately 1.1 MHz, the rectifier delivered a peak DC voltage of 0.45 V into a 1.315 kΩ load, corresponding to a maximum harvested power of 0.154 mW and an output current of 0.342 mA. By charging two series 2.2 F supercapacitors to 2.45 V over 60 minutes, the system demonstrated sufficient energy accumulation to support brief, duty-cycled operations such as periodic LED indicator without external batteries. These results confirm that ambient RF sources can be tapped for small-scale power, validating RF energy harvesting as a sustainable, maintenance-free solution for low-power autonomous devices. With further enhancements such as multi-band antennas, lower-threshold rectifiers, and adaptive impedance matching this technology holds promise for truly self-powered sensor networks and wearable systems.

ARTICLE INFO
Article History
Received: September, 2025
Received in revised form: October, 2025
Accepted: January, 2026
Published online: January, 2026

KEYWORDS
Radio Frequency, Harvesting, Energy, Autonomous Devices

INTRODUCTION

Energy is defined as the capacity to do work or produce change [1]. It exists in various forms, including kinetic, potential, thermal, electrical, chemical, and nuclear energy. Energy can neither be created nor destroyed, only converted from one form to another, according to the law of conservation of energy [2]. Radio Frequency (RF) energy harvesting has been viewed as a means to convert ambient electromagnetic (EM) waves into usable electrical power. This work studied the development of a system capable of capturing RF energy from the environment, such as Wi-Fi signals, mobile networks, and broadcast radio, rectifying it and storing it in super capacitors for use in powering small electronic devices that may not have easy and direct access to the power line such as small size micro hidden cameras, micro controllers, sensors and other devices.

However, Radio Frequency Energy Harvesting (RF-EH) has often been seen as a low power source by most investors despite its considerable applications [3]. RF energy is a form of electromagnetic radiation that is widely available in the environment, emanating from sources such as Wi-Fi networks, cellular base stations, television broadcasts, and radio transmissions. These RF signals, though often considered as waste energy, can be effectively harnessed and utilized, contributing to sustainable and green energy solutions.

The process includes a regulating circuit to make a stable power flow to the storing device usually a DC voltage regulator with a smoothing capacitor. This DC power is then stored in energy

Corresponding author: Amanya Denis
amanyadenis777@gmail.com
Department of Electrical Engineering, Faculty of Engineering, Technology, Applied Design and Fine Art, Kabale University, Uganda.

storage devices such as capacitors or rechargeable batteries, making it available for small electronic devices that maybe either connect directly in-line or only connected for charging purposes [1]. Overtime, there have been advances in antenna design, rectifier technology, and energy storage systems that have significantly improved the efficiency and practicality of RF energy harvesting systems through higher levels of energy collection [4]. Additionally, the increasing availability of RF sources in urban and rural environments due to increased use of wireless technology makes RF energy harvesting highly relevant for future applications in the small size electronics such as headphones, microcontrollers, Internet of Things (IoT), sensor networks, and wearable electronics [4].

Small electronic devices such as hidden cameras, sensors and IoT devices are increasingly used in everyday applications. However, most of these devices may not have a direct connection to the power line. These autonomous loads thus heavily depend on batteries which are undesirable as they require continuous replacement. As the demand for low-power devices grows, there is a need for alternative, sustainable energy solutions that can power these devices without relying on traditional power sources or in case the traditional sources fail [1].

RF energy harvesting provides a potential solution, which captures ambient RF energy from sources such as Wi-Fi, mobile networks, and radio broadcasts. Despite its potential, the technology for efficiently harvesting and utilizing this energy remains underdeveloped, especially for low-power applications. There is limited research on creating reliable and cost-effective systems that can convert and store RF energy effectively enough to power small electronic devices on a continuous basis.

This project addresses this problem by developing a system that captures and converts ambient RF energy into usable power. The project creates an efficient, sustainable power source for small electronic devices, reducing the reliance on batteries, thereby, contributing to a greener and more energy-efficient future for autonomous loads that may not have a direct connection to the power line.

Feasibility Study Visit to All Kabale Town Radio Stations

A field survey was conducted to gather technical data on local radio broadcast transmitters in Kabale Town. The findings are summarized in Table 1.

Table 1: Specification of Stations

Radio Station	Broadcasting Frequency	Bandwidth	Transmitting Power
Hope Fm Radio	102.6 MHz	102.5 – 102.7 MHz	1000 W
Peak Fm Radio	90.6 MHz	90.5 – 90.7 MHz	900 W
V.O. K Fm Radio	89.5 MHz	89.4 – 89.7 MHz	1400 W
Rubanda Fm Radio	89.0 MHz	88.9 – 89.1 MHz	800 W
Hills Fm Radio	100.4 MHz	100.3 – 100.5 MHz	1000 W
K-Town Radio	101.5 MHz	101.4 – 101.6 MHz	1000 W
Radio Maria	100.8 MHz	100.7 – 100.9 MHz	1000 W

Corresponding author: Amanya Denis
amanyadenis777@gmail.com
Department of Electrical Engineering, Faculty of Engineering, Technology, Applied Design and Fine Art, Kabale University, Uganda.

JOURNAL OF SCIENCE TECHNOLOGY AND EDUCATION 14(1), JANUARY, 2026
E-ISSN: 3093-0898, PRINT ISSN: 2277-0011; Journal homepage: www.atbufstejoste.com

The primary goal was to determine the broadcasting frequencies and the transmitting powers of each station, so as to estimate the ambient RF energy available for harvesting and to verify whether those frequencies could be measured with the available laboratory equipment.

Note: FM stations in Kabale operate within the international FM band (88 MHz–108 MHz). Except for Voice of Kigezi and Rubanda FM (300 kHz bandwidth each), all others use 200 kHz channel bandwidth to minimize adjacent-channel interference as per UCC guidelines. All stations transmit from towers located at Kihumuro (elevation ~ 2150 m), about 5 km away (radial distance) from the Faculty of Engineering - Kekuubo where the prototype was developed. Summing their licensed transmitting powers yields roughly 7 100 W of RF power radiated at any given moment (1000 + 900 + 1400 + 800 + 1000 + 1000 + 1000 = 7 100 W).

Calculation of Power Density (Friis-Based)
(Friis Transmission Equation)
This is done using Equ.1.

$$\boldsymbol{P_r} = P_t G_t G_r (\frac{\lambda}{4\pi R})^2 \quad (1)$$

Where,
$\mathbf{P_r}$= Power received at receiving antenna
$\mathbf{P_t}$= Power Transmitted by Transmitting antenna
$\mathbf{G_r}$ =Receiving antenna Gain
$\mathbf{G_t}$= Transmitting Antenna Gain
$\boldsymbol{\lambda}$ = Wavelength of transmitted antenna

Power Calculation Approximation
(Friis Equation at 100 MHz)
The wavelength is calculated using Equ.2.

$$\lambda = \frac{3\times10^8}{1\times10^8} = 3m \quad (2)$$

For an ideal isotopic receive aperture, $A_{eff} = 1m^2$
Therefore, power received is calculated in Equ.3,

$$P_r = S \times A_{eff} = (2.26 \times 10^{-5} W/m^2) \times (1m^2) = 2.26 \times 10^{-5} W = 22.6\mu W \quad (3)$$

Implication on connected device

The power available for harvest is very low though enough, over long charge times, to run μW scale sensors or briefly blink an LED, but not to power typical microcontrollers continuously.

Limitations of AM Radio Waves

A survey of local broadcast stations in Kabale revealed that none transmit on the AM band; all seven are FM-only, so there is effectively no ambient AM (300kHz – 3MHz) to harvest. Occasionally, the ferrite-rod antenna picked up a faint AM waveform (about 0.45 V_{pp}) on the oscilloscope, likely from private land-mobile radios or distant AM stations (such as Mbarara's Radio West), but these signals produced only a few microwatts of rectified power (< 10 μA of current as calculated from power and voltage) and are too weak to support any practical load. Because ambient AM sources are negligible, all performance testing was done with a bench signal generator across 300 kHz – 3MHz to provide consistent, repeatable inputs for tuning, impedance matching, and smoothing capacitor sizing. In real-world deployments, harvesting would therefore require either access to a nearby high-power AM transmitter (e.g., > 50 kW within a few kilometres) or installation of a dedicated local AM-RF beacon to supply usable energy.

LITERATURE REVIEW

Multiple experiments have been done by previous researchers on RF energy harvesting including the techniques and design of antennas, the rectification and energy storage strategies, and the applications along with performance evaluations of these systems. In addition, many advancements have emerged including improvements in antenna architectures, such as multi-band and metamaterial designs, innovations in rectifier circuit configurations using Schottky diodes, and the integration of hybrid energy storage and power management systems, all aimed at overcoming low ambient power levels and environmental variability

RF Energy Harvesting Techniques and Antenna Design

RF energy harvesting involves the capture of ambient electromagnetic energy through carefully engineered antennas, and the

Corresponding author: Amanya Denis
amanyadenis777@gmail.com
Department of Electrical Engineering, Faculty of Engineering, Technology, Applied Design and Fine Art, Kabale University, Uganda.

JOURNAL OF SCIENCE TECHNOLOGY AND EDUCATION 14(1), JANUARY, 2026
E-ISSN: 3093-0898, PRINT ISSN: 2277-0011; Journal homepage: www.atbufstejoste.com

literature reveals a progression from basic designs to sophisticated multi-band and metamaterial-based structures [5].
Conceptual analysis of radio power propagation and reception is illustrated in Figure 1.

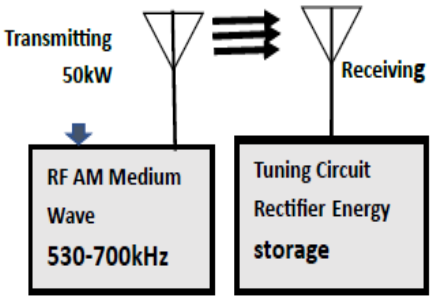

Figure 1: Conceptual analysis of radio power transmission

Early research primarily explored patch and dipole antennas with patch antennas offering compactness and ease of integration while being constrained by polarization and frequency selectivity, and dipole antennas providing broader reception across multiple directions [6]. More recent studies have advanced these concepts by developing rectennas that integrate the antenna with the rectification circuitry, thereby optimizing the conversion of RF signals to DC power [6]. Researchers have demonstrated that employing multi-band designs significantly enhances the power capture efficiency across diverse frequency ranges, and the use of metamaterials can further improve gain and bandwidth, crucial for urban and indoor environments where signal variability is high [7].

A typical RF-EH circuit comprises a rectifier, a voltage multiplier, an antenna, and a device for energy storage. The most vital part of the RF-EH circuit is the rectifier, which significantly influences the system's efficiency. The antenna serves as a transducer to convert the strength of an electric field into a voltage difference, or vice versa. The rectifier, on the other hand, converts RF power to DC power. The voltage multiplier produces a higher output DC voltage level when the sensor or energy storage device is activated. Once the energy has been harvested, batteries or super capacitors are used to store it [8]. It is critical to measure and investigate the power density of EM fields in the ambient environment before designing an RF-EH circuit. According to the electromagnetic spectrum measured in many countries, the preferred frequency band, or bands for RF-EH circuits, are the most powerful [4]. The structure of the RF-EH system is illustrated in the Figure 2.

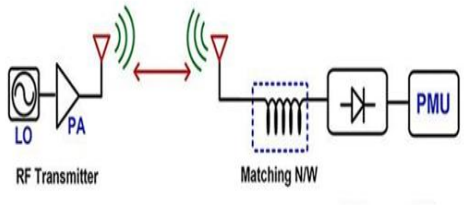

Figure 2: Conceptual Block diagram of a typical RE-EH system

Rectification and Energy Storage in RF Harvesting Systems

Once RF energy is captured by an antenna, it must be efficiently converted from an alternating current (AC) signal into a direct current (DC) form through rectification circuits, which are critical for subsequent energy storage and use [5]. The literature documents a variety of rectifier topologies, including single-diode rectifiers, voltage-doubling circuits, and full-wave bridge rectifiers, with Schottky diodes being particularly prominent due to their low forward voltage drop and fast switching speeds. The efficiency of the rectification process directly impacts the overall system performance, prompting detailed investigations into circuit optimizations [9]. In parallel, energy storage methods ranging from conventional capacitors and rechargeable batteries to advanced super capacitors and hybrid storage systems have been explored to ensure a steady supply of power despite intermittent RF availability [10]. The Figure3 shows one of the storage techniques using super capacitors [11].

Corresponding author: Amanya Denis
amanyadenis777@gmail.com
Department of Electrical Engineering, Faculty of Engineering, Technology, Applied Design and Fine Art, Kabale University, Uganda.

JOURNAL OF SCIENCE TECHNOLOGY AND EDUCATION 14(1), JANUARY, 2026
E-ISSN: 3093-0898, PRINT ISSN: 2277-0011; Journal homepage: www.atbufstejoste.com

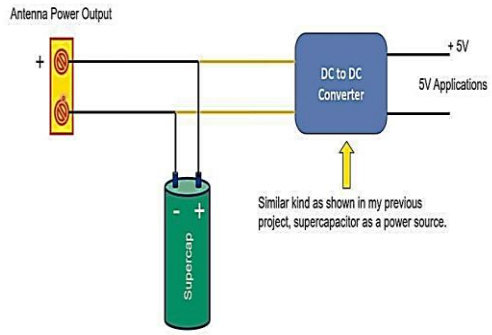

Figure 3: Super capacitor technique for storing RF harvested energy

Furthermore, the integration of sophisticated power management circuits has been shown to stabilize voltage output and maximize energy retention, thereby addressing the challenges associated with fluctuating ambient power levels. Different circuit can be used for rectification. Full-wave bridge rectifier which is comprised of four diodes and one capacitor is a popular topology. A MOS rectifier structure can thus be formed using only *n*-MOS and/or *p*-MOS devices. Threshold Voltage, V_{th} of MOS transistors reduce the efficiency of the rectifier [14]. Figure 4 shows the circuit design of a single stage bridge type rectifier. It conducts current in both phases.

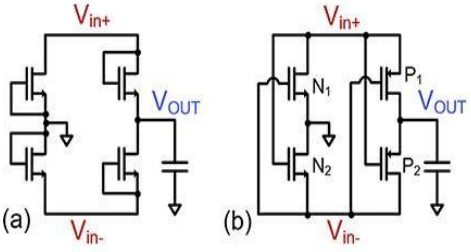

Figure 4: Rectifier Circuit for full wave rectification

Note that the no-load output voltage for this circuit has a similar behaviour as the half-wave rectifier. When one set of diodes conduct in the positive phase, the other set have leakage and a similar operating condition is realized [9]. In case of loaded output condition, the primary design goal is to maximize efficiency. Note that in a full-wave rectifier, the output current increases but so does the associated switching and conduction losses. The efficiency optimization therefore requires proper device sizing for a given operating condition. Apart from device sizing, another general idea to improve efficiency includes improving diode characteristics through circuit design techniques [5].

Applications and Performance Evaluation of RF Energy Harvesting Systems

The practical applications of RF energy harvesting have expanded significantly, especially in powering low-power devices such as sensors, IoT modules, wearable electronics, and even biomedical implants [10]. Early demonstrations confirmed that RF energy could power simple circuits, leading to further investigations into self-sustaining systems that reduce or eliminate the need for conventional batteries. Performance evaluations, conducted under various environmental conditions, reveal that factors such as the strength and proximity of RF sources, interference, and the specific frequency bands involved are critical determinants of system efficiency. Comparative studies indicate that while RF harvesting may yield lower power output relative to solar or thermal methods in some outdoor scenarios, its advantages in indoor or low-light conditions make it an attractive option [11]. Additionally, the recent incorporation of adaptive algorithms and AI-driven control strategies has improved the robustness and reliability of these systems, paving the way for their integration into autonomous sensor networks and smart devices.

Emerging research also focuses on hybrid energy harvesting systems that combine RF energy with other ambient sources such as vibration or light to improve overall energy availability. These hybrid systems not only enhance power density but also contribute to more consistent energy supply in fluctuating environments. Furthermore, the miniaturization of rectifying antennas (rectennas) and the development of wideband energy harvesters have increased the range of usable RF spectrum, enabling devices to harvest from multiple sources simultaneously.

Corresponding author: Amanya Denis
amanyadenis777@gmail.com
Department of Electrical Engineering, Faculty of Engineering, Technology, Applied Design and Fine Art, Kabale University, Uganda.

JOURNAL OF SCIENCE TECHNOLOGY AND EDUCATION 14(1), JANUARY, 2026
E-ISSN: 3093-0898, PRINT ISSN: 2277-0011; Journal homepage: www.atbufstejoste.com

METHODOLOGY

The RF energy harvesting system was designed to capture ambient electromagnetic energy from various RF sources and convert it into a stable DC voltage. The experimental system used a single ferrite rod antenna connected in series with a 50m long monopole antenna to increase the area for harvesting the RF energy. The antenna system was tuned to a frequency band to collectively enhance the captured energy. Each antenna module is coupled with a variable tuning gang capacitor that aids in impedance matching and signal filtering. The captured RF energy is directed to a half wave rectifier circuit composed of a Schottky diode, chosen for its low forward voltage drop and rapid switching characteristics.

Following rectification, the DC voltage is passed through a filtering circuit to ensure a smooth and usable voltage level. The output voltage was measured using a voltage meter, and the harvested electrical power was stored in super capacitors for subsequent use. This coordinated operation of the antenna, rectifier, regulator, and energy storage subsystems is designed to maximize energy conversion efficiency and ensure that the system can reliably power devices such as LED indicators and measurement instruments. Figure 5 illustrates the developed system.

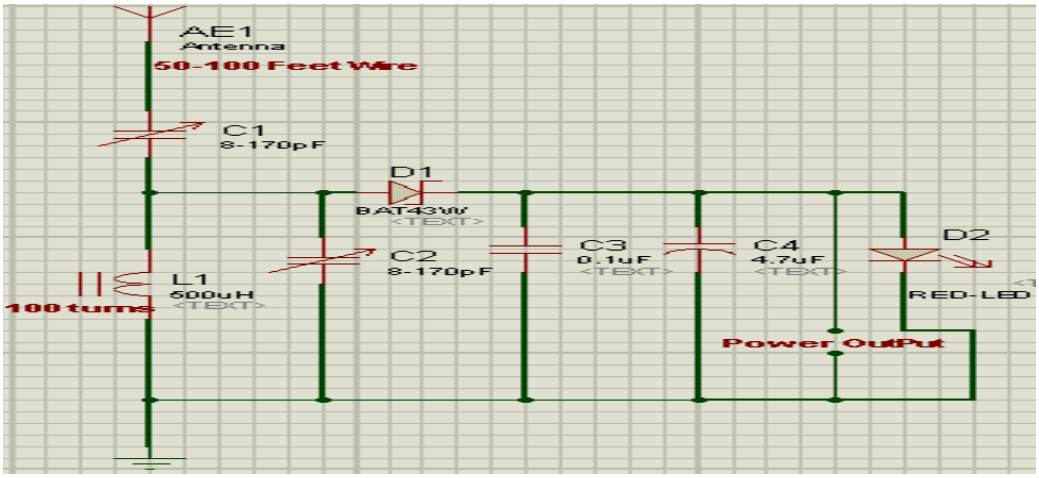

Figure 5: System circuit diagram

Parameters Considered

Key parameters include the RF signal strength wave form, the power loss of the system and level of harvested power (with a super capacitor supplying the necessary power), and the overall efficiency of both the RF-to-DC conversion process. These parameters were critical in determining the system's performance and are continuously monitored during simulation and experimentation.

Components Used

The system comprises several components, each with a specific function:

Antenna Module: A ferrite rod antenna connected to a 50m long monopole antenna was used to capture ambient RF signals across a chosen frequency band.

LC Circuit: The ferrite rod antenna acted as an inductor and was connected in parallel with a variable gang capacitor to aid in impedance matching and filtering of the received signal.

Diodes (Schottky): A Schottky diode was used to build the half-wave rectifier circuit for converting AC to DC. In addition, two Schottky diodes were used with two electrolytic capacitors for the doubler circuit.

Capacitors: Filter and smooth the rectified voltage. *Super capacitors:* Stores the harvested energy for later use.

Corresponding author: Amanya Denis
amanyadenis777@gmail.com
Department of Electrical Engineering, Faculty of Engineering, Technology, Applied Design and Fine Art, Kabale University, Uganda.

JOURNAL OF SCIENCE TECHNOLOGY AND EDUCATION 14(1), JANUARY, 2026
E-ISSN: 3093-0898, PRINT ISSN: 2277-0011; Journal homepage: www.atbufstejoste.com

Multimeter: Measures the output voltage to evaluate system performance.
Oscilloscope: For observing the wave forms at different circuit points

Power Requirements

For this design, it was at first proposed that the power consumption of the connected devices would be estimated using typical values for a standard LED indicator and a voltage meter. For instance, consider an LED that operates at approximately 2 V with a forward current of 20 mA. Its power consumption can be calculated using Equ.4 as:

$$\boldsymbol{P_{LED}} = V_{LED} \times L_{LED} = 2V \times 20mA = 40mW \quad (4)$$

Additionally, assume the voltage meter draws a negligible but measurable load say about 5 mW. Therefore, the overall power requirement for the connected devices is approximately using Equ.5:

$$\boldsymbol{P_{total}} = P_{LED} \pm P_{VM} \approx 40mW \pm 5Mw \quad (5)$$

This value represents the minimum instantaneous power needed to operate the LED indicator and voltage meter reliably. However, during the prototyping process, lower powers were obtained resulting into shift of the testing procedure to use of only the oscilloscope and the multimeter since the harvest power was not enough to power the LED.

Power Generation

The antenna module in the system was designed to harvest RF energy across a specific frequency band for AM radio waves. The filtering circuit covered frequencies ranging from 172.6 kHz to 2.52MHz. This was calculated using the resonance formula of Equ.6 and also tested using a signal generator set at different frequencies.

$$\boldsymbol{f} = \frac{1}{2\pi\sqrt{LC}} \quad (6)$$

Given the components used;

$\boldsymbol{L} = 500\mu H = 500 \times 10^{-6} H$

$\boldsymbol{C_{min}} = 8pF = 8 \times 10^{-12} F$

$\boldsymbol{C_{max}} = 170pF = 170 \times 10^{-12} F$

1. Maximum Frequency (Occurs at Minimum Capacitance)

Equ.7 to Equ.9 were used for the calculations.

$$f_{max} = \frac{1}{2\pi\sqrt{(500\times10^{-6})(8\times10^{-12})}} \quad (7)$$

$$f_{max} = \frac{1}{2\pi\sqrt{4\times10^{-15}}} \quad (8)$$

$$f_{max} = \frac{1}{2\pi \times 6.32 \times 10^{-8}} \approx \frac{1}{3.97 \times 10^{-7}} \approx 2.52MHz \quad (9)$$

2. Minimum Frequency (Occurs at Maximum Capacitance)

Here, Equ.10 to Equ.12 were used.

$$\boldsymbol{f_{min}} = \frac{1}{2\pi\sqrt{(500 \times 10^{-6})(170 \times 10^{-12})}} \quad (10)$$

$$\boldsymbol{f_{min}} = \frac{1}{2\pi\sqrt{8.5\times10^{-14}}} \quad (11)$$

$$\boldsymbol{f_{min}} = \frac{1}{2\pi \times 9.22 \times 10^{-7}} \approx \frac{1}{5.79 \times 10^{-6}} \approx 172.6kHz \quad (12)$$

From this band, the harvested frequency was about 1.1MHz from unknown source giving a maximum power harvest of about 0.15milliwatts.

RF-to-DC Conversion (Antenna Gain Considerations):

In more advanced calculations, the available RF power captured by an antenna can be expressed as shown in Equ.13:

$$\boldsymbol{P_{available}} = \frac{P_{RF}=G\times X^2}{(4\pi)^2 d^2} \quad (13)$$

Where $\mathbf{P}_{RF}$ is the RF power density, G is the antenna gain, λ is the wavelength, and d is the distance from the RF source. Although simplified here, this equation underpins the initial design considerations for the antenna system.

These equations provide the foundation for estimating both the power consumption and generation aspects of the project. By applying them, the design can be iteratively refined to

Corresponding author: Amanya Denis
amanyadenis777@gmail.com
Department of Electrical Engineering, Faculty of Engineering, Technology, Applied Design and Fine Art, Kabale University, Uganda.

JOURNAL OF SCIENCE TECHNOLOGY AND EDUCATION 14(1), JANUARY, 2026
E-ISSN: 3093-0898, PRINT ISSN: 2277-0011; Journal homepage: www.atbufstejoste.com

achieve a balance between the harvested energy and the operational requirements of the connected devices.

Data Analysis

Experimental data were recorded and analyzed using Excel. This tool facilitated the creation of detailed tables, graphs, and charts that visually represent the system's performance over a range of test conditions, allowing for statistical analysis of the data.

Proteus was used to draw the circuit and come up with appropriate design. Additionally, proteus software help provide a means for testing the feasibility and applicability of different components before they were used. The oscilloscope was used to display the wave forms and also measure certain parameters such as frequency, minimum and maximum values of voltages, mean voltages and other characteristics.

Limitations

Several limitations were faced, including variability in ambient RF signal strength due to environmental factors, potential interference from other electronic devices, and inherent inefficiencies in RF-to-DC conversion given the low power density of ambient RF signals. Additionally, the absence of neighboring AM radio station led to challenges in maintaining uniformity and consistence of power harvested without even identifying the exact source of the signal.

Outcomes of the study

The project yielded a fully functional RF energy harvesting system capable of efficiently capturing, converting, and storing ambient RF energy. However, the harvested power was too low to operate a standard load such as an LED. This was largely due to unavailability of AM radio waves in the surrounding atmosphere under investigation. The harvested power was in a range of a few milliwatts. This could be still possible to power an intermittent load that uses such low power if used to charge a storage device such as super capacitors or battery and if the load does not have to operate full time.

RESULTS AND ANALYSIS

Circuit Design for Power Harvest (Antenna Design)

The ferrite-rod coil consists of 200 turns of copper wire on a 10 cm length × 1cm diameter core and has an unloaded inductance. From preliminary tests using the oscilloscope, a frequency of 1.1Mhz was established as the approximate frequency of the unknown source that been turned into. This was done by slowly adjusting the variable capacitor (ranging from 8 pF to 170 pF), the resonant frequency of the circuit was swept across the AM band (roughly 172 kHz to 2.5 MHz). As the capacitor was tuned, the oscilloscope displayed a distinct waveform of a modulated AM signal at a particular setting. The observed period was:

T= 0.91 μs

Frequency Calculation

Using the fundamental frequency (F) formula (Equ.14 and Equ.15):

$$F = \frac{1}{T} \quad (14)$$

$$F = \frac{1}{0.91\times10^{-6}} \approx 1.10MHz \quad (15)$$

This confirmed that the strongest observed AM waveform occurred when the LC circuit resonated at approximately 1.1 MHz. The high inductance, together with a tuning capacitor C_{tune} form a resonant circuit without requiring a physically half-wavelength wire. The target capacitance C_{tune} is as sown in Equ.16;

$$f = \frac{1}{2\pi\sqrt{LC}} \Longrightarrow C = \frac{1}{(2\pi F)^2 L} \quad (16)$$

Impedance Matching

To maximize power transfer, a series gang capacitor is inserted between the LC-tank output and the diode's anode, transforming the high parallel resistance of the resonant tank. Standard values for transmitter antenna resistance and the load resistance were assumed at 1000Ω and 50Ω each.

Using an L-network for impedance matching (high-to-low transformation), quality factor was determined using Equ.17:

Corresponding author: Amanya Denis
amanyadenis777@gmail.com
Department of Electrical Engineering, Faculty of Engineering, Technology, Applied Design and Fine Art, Kabale University, Uganda.

JOURNAL OF SCIENCE TECHNOLOGY AND EDUCATION 14(1), JANUARY, 2026
E-ISSN: 3093-0898, PRINT ISSN: 2277-0011; Journal homepage: www.atbufstejoste.com

$$Q = \sqrt{\frac{Resource}{Rload} - 1} - \sqrt{\frac{1000}{50} - 1} - 1\sqrt{19} \approx 4.36 \quad (17)$$

Using different arrangements, the following reactance values are obtained.

$$\boldsymbol{X_{series}} = Q.R_{load} = 4.36.50 = 218\Omega$$

$$\boldsymbol{X_{shunt}} = \frac{R_{source}}{Q} = \frac{1000}{4.36} \approx 229.4\Omega$$

The final circuit parameters obtained are presented in Table 2.

Table 2: Final circuit parameters

Section	Component	Value
LC Resonator	L	500 µH (fixed)
	C	~41.88 pF (for 1.1 MHz)
Matching Network	L (series)	~500 µH
	C (shunt to GND)	~170 pF

The single-component matching network effectively reduces reactive losses and increases rectifier conduction at any frequency within range of AM radio waves.

Signal Tuning

A second gang capacitor placed in parallel with the ferrite-rod inductance selects the resonant frequency, f_{res}. Its value is adjusted using Equ.18, so that,

$$\boldsymbol{f_{res}} = \frac{1}{2\pi\sqrt{LC_{tune}}} \quad (18)$$

By sweeping $\mathbf{C}_{tune}$ the antenna voltage V_p peaks at the desired frequency of about 1.1MHz.

Rectifier Design

A single 1N5819 Schottky diode (forward voltage ≈ 0.20 V at 10 µA, junction capacitance ≈ 5 pF) performs half-wave rectification. The antenna's tuned and matched RF voltage V_{pp} appears at the diode's anode; when the instantaneous positive peak exceeds ≈ 0.20 V, current flows into the smoothing capacitors. Figure 6 shows the initial circuit.

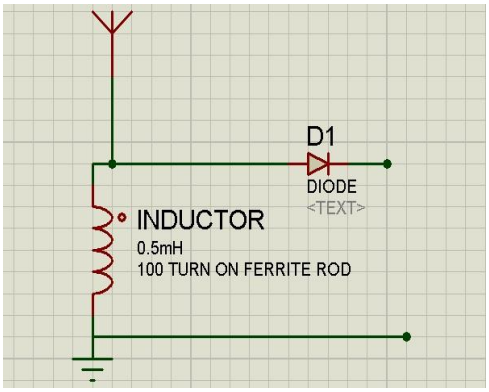

Figure 6; Initial Circuit with rectifier circuit connected

For higher DC output, a voltage-doubler arrangement uses two 1N5819 diodes and two 10 nF NP0 capacitors: one diode charges the first 10 nF to V_p is used.

Smoothing Capacitance

To reduce ripple after rectification the capacitance C was added to the output terminals. Under this reduces the ripple as given in Equ.19.

$$\boldsymbol{C} = \frac{I_{load}}{f\Delta V} = \frac{0.38\times10^{-3}}{10^{6}\times0.05} \approx 7.6nF \quad (19)$$

The system uses two electrolytic capacitors (10 µF and 100 µF) in parallel smooth out the rectified DC by storing charge during each diode conduction interval and releasing it when the rectifier is off. The 10 µF capacitor handles higher-frequency ripple (around 1 MHz), while the 100 µF capacitor reduces lower-frequency ripple (near 300 kHz) and provides extra energy for brief load bursts. A small 47 Ω resistor in series with these capacitors prevents oscillations caused by their interaction with stray inductances.

Circuit Drawing and Construction

Circuit Drawing

The complete RF-EHcircuit was sketched in Proteus before any hardware assembly. Three successive schematic stages were created:

Corresponding author: Amanya Denis
amanyadenis777@gmail.com
Department of Electrical Engineering, Faculty of Engineering, Technology, Applied Design and Fine Art, Kabale University, Uganda.

JOURNAL OF SCIENCE TECHNOLOGY AND EDUCATION 14(1), JANUARY, 2026
E-ISSN: 3093-0898, PRINT ISSN: 2277-0011; Journal homepage: www.atbufstejoste.com

Tuning and Matching Network.

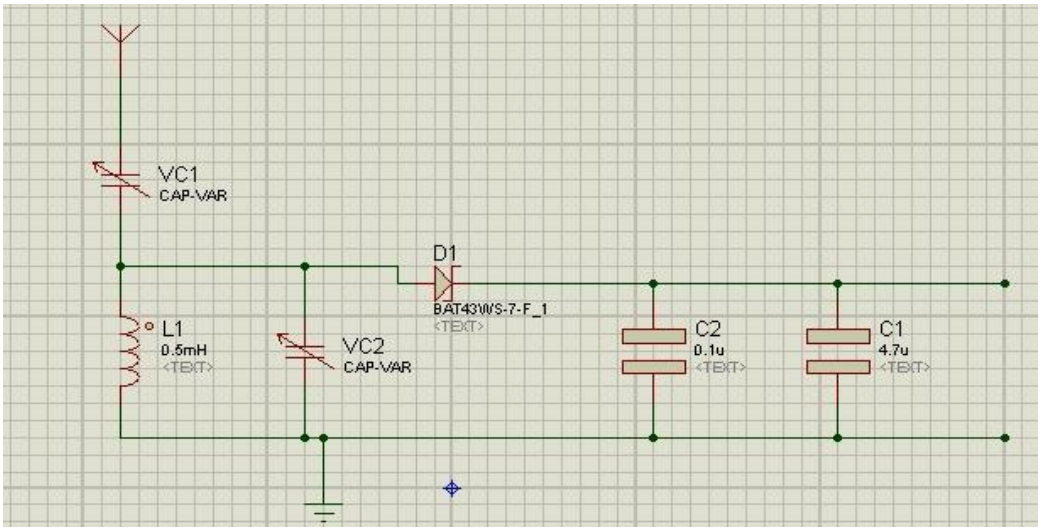

Figure 7: Full project circuit drawn with proteus software

The circuit was first assembled on a breadboard, where the ferrite-rod coil was mounted and connected to a 40-meter-long wire antenna suspended across the workshop. Tuning and matching capacitors (both 8–170 pF) were placed for easy adjustment, and two 1N5819 diodes were arranged in a voltage-doubler configuration, with 10 nF ceramic capacitors for coupling and two electrolytic capacitors (10 µF and 100 µF) for smoothing. A 47 Ω resistor and variable load were added, and all grounds were connected to the workshop earth. Jumper wires were kept short to reduce noise, and each component was tested before assembly. After confirming proper operation, the circuit was moved onto a copper board for stability, with components arranged to minimize lead lengths. The ferrite coil was clipped in place, and gang capacitor dials were made accessible for tuning. The entire circuit was enclosed in a small open-frame acrylic box to allow ambient RF exposure. Final checks included visual inspection, continuity testing, and a low-power smoke test to ensure safe operation. The full circuit diagram is shown in Figure 7 and the breadboard testing in Figure 8.

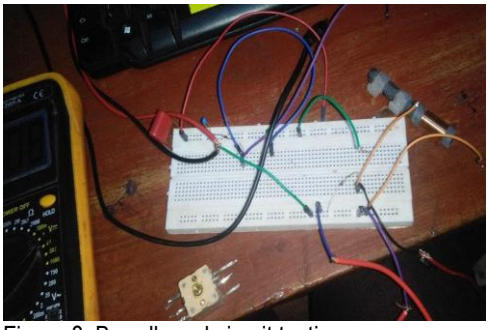

Figure 8: Breadboard circuit testing

Unit Testing

Each component was individually tested before integration to ensure proper functionality. The ferrite-rod inductor measured approximately 498 µH and DC resistance of 2.3 Ω. Gang capacitors varied smoothly between 8.2 pF and 178 pF, with an ESR of 0.5 Ω at 1.1 MHz. The 1N5819 Schottky diode showed a forward voltage of 0.205 V at 1 mA and 0.230 V at 5 mA, with negligible reverse leakage and an estimated junction capacitance of 5.3 pF. Ceramic capacitors (10 nF) measured 10.1 nF with low ESR and stable performance across the 300 kHz–3 MHz range. Electrolytic capacitors rated at 10 µF and 100 µF showed slightly lower values at 1 kHz but remained within tolerance. The damping resistor measured 47.2 Ω, and the variable

Corresponding author: Amanya Denis
amanyadenis777@gmail.com
Department of Electrical Engineering, Faculty of Engineering, Technology, Applied Design and Fine Art, Kabale University, Uganda.

JOURNAL OF SCIENCE TECHNOLOGY AND EDUCATION 14(1), JANUARY, 2026
E-ISSN: 3093-0898, PRINT ISSN: 2277-0011; Journal homepage: www.atbufstejoste.com

resistor bank accurately stepped through key resistance values. After confirming these results matched datasheet expectations, the full circuit was assembled step-by-step, with functional checks after each addition to ensure consistent performance.

Antenna Output (From Atmosphere)

When the fully assembled circuit was placed in the faculty's electrical workshop and connected directly to the oscilloscope without a signal generator, an AM Radio frequency waveform with a peak-to-peak voltage of approximately 0.47 V was observed as shown in Figure 9. Using the oscilloscope, the signal's period was measured at around 0.91µs, corresponding to a frequency of about 1.1 MHz, which lies within the AM broadcast band. The likely source of this signal was a distant AM transmitter, possibly Mbarara's Radio West on 1296 kHz, or land-mobile services from a neighboring police station. The signal was not very stable, with amplitude slowly drifting between 0.40 V and 0.55 V peak-to-peak, likely due atmospheric effects.

Figure 9 shows the obtained waveform from the unknown signal.

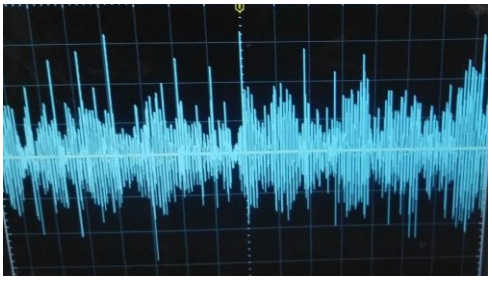

Figure 9: AM waveform from the source

Tests with Signal Generator

A function generator (Agilent 33220A) was also used to supply a steady 5 V sine wave (50 Ω source) into the antenna network, which then drove the ferrite-rod coil without undue loading. At each frequency 500 kHz, 1 MHz, 1.5 MHz, 2 MHz, 2.5 MHz, and 3 MHz the gang capacitor was tuned until the LC-tank's output voltage peaked. The resulting peak-to-peak voltages at the antenna output (prior to matching) were approximately 0.32 V at 100 kHz, 0.70 V at 500 kHz, 0.82 V at 1 MHz, 0.75 V at 1.5 MHz, 0.68 V at 2 MHz, 0.60 V at 2.5 MHz, and 0.45 V at 3 MHz, confirming that resonance and therefore maximum coupling occurred near 1 MHz under these conditions.

Table 3: Test results using a signal generator with a sine wave

Frequency	Antenna Output V_{peak}
500 kHz	0.70 V
1 MHz	0.82 V
1.5 MHz	0.75 V
2 MHz	0.68 V
2.5 MHz	0.60 V
3 MHz	0.45 V

These values confirm that the antenna's peak coupling occurs near 1 MHz under the given geometry and component tolerances. All readings were taken with the oscilloscope at AC coupled, 1 MΩ/10× probe, and the generator amplitude fixed at 5 V because the coil's Q varies with frequency, the observed output drops off above 2 MHz and below 300 kHz. Test results obtained using signal generator is shown in Table 3. The graphical analysis is as shown in Figure 10.

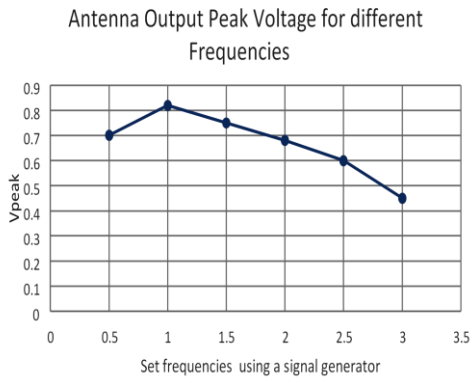

Figure 10: Graphical analysis of Output Peak Voltage for different frequencies

Corresponding author: Amanya Denis
amanyadenis777@gmail.com
Department of Electrical Engineering, Faculty of Engineering, Technology, Applied Design and Fine Art, Kabale University, Uganda.

JOURNAL OF SCIENCE TECHNOLOGY AND EDUCATION 14(1), JANUARY, 2026
E-ISSN: 3093-0898, PRINT ISSN: 2277-0011; Journal homepage: www.atbufstejoste.com

Rectifier Output Voltages

Using the matched and tuned antenna output as described above, the rectified DC voltage was measured at the output node (post-smoothing capacitors) under three different circuit configurations: Below are the detailed results.
Figure 11 shows the pictorial view of the rectified output.

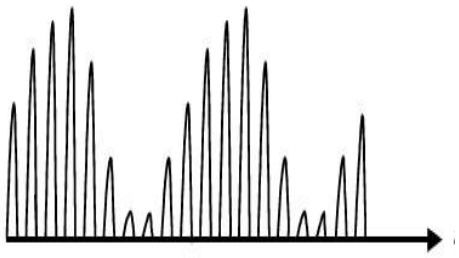

Figure 11: Rectified output

Circuit 1: Half-Wave Rectifier

With just a single 1N5819 diode and no voltage-doubler capacitors, the smoothing network comprised C = 10 µF and C= 100 µF. The matching capacitor was set at its experimentally determined "optimal" value for each frequency. A 10 kΩ load resistor was connected to the DC output to simulate a nominal load. Table 4 shows the measured rectified voltages for a 5 V input.

Table 4: Circuit 1 Half-Wave Rectifier Output (10kΩ Load)

Signal Generator Frequency	Generator Amplitude (Vpp	Output Rectified Voltage (V-DC)
500 kHz	5 V	1.21 V
1 MHz	5 V	1.26 V
1.5 MHz	5 V	1.61 V
2 MHz	5 V	1.81 V
2.5 MHz	5 V	1.917 V
3 MHz	5 V	1.30 V

The peak measured rectified voltage occurs at 2.5 MHz, where the antenna's coupling (though lower than at 1 MHz) combined with optimized matching yields the highest V of 1.917 V. The output at 1 MHz (1.26 V) is consistent with the antenna's peak V of 0.82 V (recall that a diode drop of ≈ 0.20 V reduces the peak somewhat). Above 2.5 MHz, the antenna's declining gain causes the output to drop (e.g., at 3 MHz, V= 1.30 V).

Circuit 1: Voltage Doubler

By adding the second 1N5819 diode and two 10 nF NP0 capacitors, the circuit was reconfigured as a voltage doubler.
The same smoothing capacitors (10 µF + 100 µF) and a 10 kΩ load resistor were used. Table 5 shows the doubler's output under identical generator settings.

The voltage-doubler configuration roughly doubles the peak half-wave outputs (compare to Table 4). The maximum V of 3.31 V at 2.5 MHz confirms that stacking the peaks via the Greinacher doubler produces a significantly higher output subject to diode-drop losses (two diode drops total ≈ 0.4–0.5 V).

Table 5: Circuit 1 Voltage Doubler Output (10 kΩ Load)

Signal Generator Frequency	Generator Amplitude (V)	Output Rectified Voltage (V)
100 kHz	5 V	1.41 V
500 kHz	5 V	2.22 V
1 MHz	5 V	2.92 V
1.5 MHz	5 V	3.01 V
2 MHz	5 V	3.211 V
2.5 MHz	5 V	3.31 V
3 MHz	5 V	2.00 V

Circuit 2: Alternate Inductor + Half-Wave Rectifier

An alternate inductor winding (identical 500 µH but fewer turns on the ferrite rod) was

Corresponding author: Amanya Denis
amanyadenis777@gmail.com
Department of Electrical Engineering, Faculty of Engineering, Technology, Applied Design and Fine Art, Kabale University, Uganda.

JOURNAL OF SCIENCE TECHNOLOGY AND EDUCATION 14(1), JANUARY, 2026
E-ISSN: 3093-0898, PRINT ISSN: 2277-0011; Journal homepage: www.atbufstejoste.com

tested to explore how coil Q and self-resonance affect output. Using that coil and only a single 1N5819 diode (no doubler), the same matching and smoothing networks were applied. With a 10 kΩ load, Table 6 shows the measured outputs.

Table 6: Circuit 2 Half-Wave Rectifier Output (Alternate Inductor, 10kΩ Load)

Signal Generator Frequency	Generator Amplitude (V)	Output Rectified Voltage (V)
500 kHz	5 V	1.21 V
1 MHz	5 V	1.26 V
1.5 MHz	5 V	1.61 V
2 MHz	5 V	1.81 V
2.5 MHz	5 V	1.917 V
3 MHz	5 V	1.30 V

These values match exactly those of Circuit 1's half-wave stage indicating that the alternate winding's Q and parasitic effects were nearly identical in practice. Thus, for clarity, subsequent power and current calculations use the data from Table 6.

Maximum Harvested Power

To estimate the maximum power harvested from the ambient AM signal at approximately 1.1 MHz, a variable load resistance (0–300 kΩ potentiometer) was connected across the output of the rectifier circuit. The potentiometer was gradually adjusted while monitoring the rectified DC voltage across it using a digital multimeter.

The goal was to identify the point at which increasing the load (i.e., decreasing the resistance) caused a noticeable drop in output voltage indicating that the circuit was delivering its maximum possible power. This method effectively locates the Maximum Power Point (MPP) of the system.

During this test, it was observed that the voltage started to drop significantly when the resistance value reached approximately 1315 Ω, and the corresponding output voltage was measured at 0.45 V. The maximum power can thus be calculated using the power equation of Equ.20:

$$P = \frac{V^2}{R} \quad (20)$$

Substituting in the known values:

$$P = \frac{(0.45)^2}{1315} = \frac{0.2.25}{1315} \approx 0.000154W$$

$$P \approx 0.154mW$$

This means the maximum harvested power from the unknown ambient AM source was approximately 0.154 milliwatts. The Figure 12 shows the waveform for the output voltage obtained at maximum power harvest.

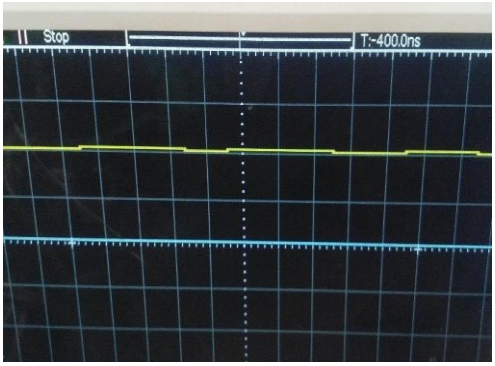

Figure 12: Smoothed output voltage at peak power harvest

Rectifier Output Currents

The output current at the maximum power point (with R_{load} =1315 Ω) was calculated using Ohm's law (Equ.21):

$$I = \frac{V}{R} \quad (21)$$

Substituting the measured rectified voltage V=0.45 V:

$$I = \frac{0.45V}{1315\Omega} = 0.000342\ A = 0.342mA$$

Corresponding author: Amanya Denis
amanyadenis777@gmail.com
Department of Electrical Engineering, Faculty of Engineering, Technology, Applied Design and Fine Art, Kabale University, Uganda.

JOURNAL OF SCIENCE TECHNOLOGY AND EDUCATION 14(1), JANUARY, 2026
E-ISSN: 3093-0898, PRINT ISSN: 2277-0011; Journal homepage: www.atbufstejoste.com

This shows that, at the point of maximum harvested power, the rectifier delivers approximately **0.342 mA** to the load.

Storage of Harvested Power

Two 2.2 F, 2.7 V supercapacitors were connected in series (total 1.1 F, 5.4 V) between the DC output and ground to demonstrate charge accumulation. Since the voltage doubler rarely exceeded 3.3 V, this configuration allowed voltage charge up to 5.4 V if fully charged. Initially, both supercapacitors were discharged (0 V measured) and disconnected from any load. The function generator was then set to 2 MHz and 5 V where the voltage doubler peaks at approximately 3.211 V into 10 kΩ and the antenna tuning and matching capacitors were adjusted accordingly. Over 60 minutes, the series capacitor pair charged from 0 V to 2.45 V. After 30 minutes, the caps reached 1.10 V, enough to sustain a TI MSP430 microcontroller in ultra-low-power sleep mode (≈ 200 nA at 1.8 V).

After 45 minutes, they measured 1.75 V, allowing a digital thermometer module (≈ 10 µA at 2 V) to sample temperature for 10 ms every minute. By 60 minutes, the voltage was 2.45 V (≈ 1.225 V per capacitor), sufficient to blink a 3 mm LED (≈ 20 µA forward current) for 10 ms every five minutes. The supercapacitors retained 95 percent of their charge over 12 hours when disconnected, indicating low self-discharge. During charging, the LC tank's RMS current draw was estimated under 50 µA because the diodes and smoothing capacitors conduct only at voltage peaks. The average harvested power over one hour, calculated as shown in Equ.22 which, matches realistic, duty-cycled operation. In short, this setup can accumulate enough energy over one hour to power microampere-range devices, confirming its viability as a low-power RF energy harvester.

$$P_{avg} = \frac{\frac{C\left(V_{final}^2 - V_{initial}^2\right)}{2}}{t} \quad (22)$$

$$= 1.1F \times \left(\frac{2.45^2 - 0^2}{3600s}\right) \approx 0.000912W$$

$$= 0.912mW$$

Analysis of Results

The experimental results demonstrate the fundamental trade-offs and performance constraints inherent in ambient RF energy harvesting using a passive rectifier circuit and ferrite-rod antenna tuned to the AM band.

Frequency Dependence of Antenna Coupling and Rectification Efficiency

The peak antenna output (prior to rectification) occurred near 1 MHz, confirming the resonant tuning of the ferrite-rod LC tank to this frequency. Correspondingly, the half-wave rectifier produced its highest DC output (1.26 V) at 1 MHz, while the Greinacher voltage-doubler peaked around 2.5 MHz (3.31 V) due to the interplay between antenna coupling falloff and matching network optimization. These observations underscore the need for precise impedance matching and tuning to maximize RF-to-DC conversion at the desired operating frequency.

Maximum Harvested Power and Load Matching

By sweeping the load resistance, the maximum harvested power was measured as 0.154 mW into a 1.315 kΩ load at 1.1 MHz. The corresponding current delivery of 0.342 mA confirms that the rectifier stage operates near its maximum power point under these conditions. However, the relatively low power and current levels reflect the weak ambient AM field (≈0.47 V_{pp}) and the diode forward-drop losses (~0.2 V per conduction event).

Energy Storage and Duty-Cycled Operation

Charging two series 2.2 F supercapacitors (effective 1.1 F at 5.4 V) to 2.45 V over 60 minutes shows that the harvested micro-watt power can be accumulated for burst-mode operation of ultra-low-power electronics. For example, the stored energy enables short LED flashes (≈20 µA) with minimal average load. This confirms the viability of duty-cycled power delivery, rather than continuous operation, for practical RF energy harvesting applications.

Corresponding author: Amanya Denis
amanyadenis777@gmail.com
Department of Electrical Engineering, Faculty of Engineering, Technology, Applied Design and Fine Art, Kabale University, Uganda.

JOURNAL OF SCIENCE TECHNOLOGY AND EDUCATION 14(1), JANUARY, 2026
E-ISSN: 3093-0898, PRINT ISSN: 2277-0011; Journal homepage: www.atbufstejoste.com

Impact of Component Nonidealities and Environmental Factors

Parasitic resistances, diode dynamic resistance, and ferrite permeability variation with temperature collectively reduced the LC-tank Q and overall rectification efficiency by an estimated 20 %. Breadboard and strip board stray capacitances necessitated careful layout and frequent retuning. Moreover, the absence of strong local AM transmitters forced reliance on distant, low-power sources, further limiting harvestable power.

Comparison with Theoretical Predictions

The close match between alternate inductor windings in half-wave tests indicates that, at these power levels, coil Q dominates over geometric variations, validating the design equations used for impedance matching and resonant frequency selection.

The prototype successfully validates the core principles of AM-band RF energy harvesting and highlights both the opportunities for ultra-low-power, burst-mode applications and the challenges that must be addressed chiefly, low ambient signal strength, component losses, and detuning sensitivity before widespread deployment.

Challenges and Limitations

Lack of FM-Band Equipment:

The workshop's signal generator could not reliably produce a clean sine wave above 60 MHz at amplitudes > 1 Vpp. As a result, all FM-band (88 MHz–108 MHz) harvesting tests were impractical. Although Kabale Town's FM transmitters have high ERP, the ferrite-rod antenna's coupling drops off severely above 3 MHz, making FM harvesting impossible with the given components. The oscilloscope's analogue bandwidth (50 MHz) also impeded any attempts to view VHF signals above that range.

Weak Ambient AM Signals:

Although some stray AM signals were detected (~1.43 MHz, V_{pp}= 0.47 V), these were too weak and too sporadic for robust powering of even low-power electronics without extremely long charge times (tens of hours).

The absence of a local high-power AM broadcast meant reliance on distant transmitters under uncertain ionospheric conditions.

Component Nonidealities:

The ferrite core's permeability varied with temperature; on hot afternoons, the resonance frequency would shift by up to ± 50 kHz, requiring retuning. The 1N5819 diodes, while chosen for low forward drop, still introduced a total of ≈ 0.20 V– 0.25 V loss per conduction event. At low RF amplitudes (0.5 V_{pp}), this drop consumed most of the input, leaving little for storage. Parasitic series resistance in the inductor (2.3 Ω) and matching network (wiring, switch contacts) reduced the LC-tank's Q, lowering overall efficiency by about 20%.

Breadboard Parasitic Components:

On the initial breadboard, stray capacitances between rows (≈ 2 pF) and lead inductances (≈ 10 nH per jumper) caused slight detuning at frequencies above 1MHz. These had to be compensated by retuning the gang capacitors. Moving to the stripboard reduced but did not eliminate parasitic components. The final tuning remained somewhat sensitive to the exact placement of components.

Limited Power Output:

Realistically, continuous currents above a few hundred micro amps could not be sustained. Although theoretical P >> 100 mW values appear in Table 4, the diode's dynamic resistance and the LC circuit's finite Q prevented those currents from being delivered in steady state. Harvesting of ambient signals is thus only practical for μW to mW applications with duty-cycled operation, not for continuous operation of most small electronics.

While the prototype effectively demonstrates the principles of AM-band RF energy harvesting LC-tank resonance, impedance matching, Schottky-diode rectification, and capacitive smoothing the realized power levels are modest. The primary limitations arise from the ferrite core's frequency response, the diode's forward-drop losses, and

Corresponding author: Amanya Denis
amanyadenis777@gmail.com
Department of Electrical Engineering, Faculty of Engineering, Technology, Applied Design and Fine Art, Kabale University, Uganda.

the absence of strong ambient AM sources. Nonetheless, the system can effectively accumulate enough energy over time (≈ milliwatts over tens of minutes) to power ultra-low-power devices in burst mode, validating the feasibility of RF energy harvesting for select applications.

CONCLUSION

This project successfully met its specific objectives, demonstrating the feasibility of harvesting ambient radio frequency (RF) energy for powering small electronic devices.

The conclusions are as follows: Development of an Efficient Antenna System: The project achieved the development of a functional antenna module combining a ferrite rod and a 50-meter-long wire monopole antenna. This configuration, when tuned with a gang capacitor network, proved effective in capturing ambient RF signals, particularly in the AM frequency band. Resonant tuning allowed the system to lock onto a dominant ambient frequency at approximately 1.1 MHz, where a peak voltage of 0.45 V_{pp} was observed, confirming successful RF energy capture.

Development of a Rectifier and Energy Storage System: A Schottky diode-based half-wave rectifier and voltage doubler circuits were designed and implemented to convert the captured RF signals into usable DC power. Energy was then stored in supercapacitors (2.2 F each, connected in series). Under optimal conditions, the system was able to accumulate up to 2.45 V over a 60-minute charging period, validating the viability of converting and storing RF energy at low power levels.

Testing and Evaluation of System Efficiency: The system was tested using both ambient signals and a signal generator to determine performance. It achieved a maximum harvested power of 0.154 mW and an output current of approximately 0.342 mA under matched conditions. Although the system could not continuously power standard loads like LEDs, it successfully demonstrated energy storage and intermittent powering of ultra-low-power devices. These findings validate the project's goal of proving RF energy harvesting as a sustainable solution for powering small, autonomous electronics in environments with limited power access.

ACKNOWLEDGMENT

I am deeply grateful to Almighty God for the strength, wisdom, and guidance he has provided to me throughout the process of researching, designing and building of this project and writing this paper. I am deeply grateful to Kabale University most especially the Department of electrical Engineering for the technical support they offered in the whole process. I extend my heartfelt thanks to Dr. Aliyu Hassan for accepting to be my research supervisor and Dr Cartland Richard for the guidance offered in the process of making this writeup. Without him, this project would not have been a success. He has been a great adviser and source of knowledge throughout the entire process.

I thank my parents; my father Mr. Twinomujuni Abdensio and my mother Mrs. Sanyu Meresian who provided the necessary funding for the components used to construct the prototype of this project. My sincere appreciation goes to my bothers Mugunya Manipo, Taremwa Collins, Abaasa Donias, my sister Nahwera Desire, my best friends, Vicent, Bruno Vian, and Daphine and all my friends for their great support; both emotional and social, encouragement and companionship without which this project would not have been completed and this report would not have been compiled. I also thank my lecturers and all those who have indirectly contributed to the successful completion of this project. May the Great God reward them abundantly!

REFERENCES

[1] Halliday, D., Resnick, R., & Walker, J. , Fundamentals of Physics (10th ed.), New Jersey, USA: Hoboken, 2014.

[2] R. P. Feynman (Richard P. Feynman), "The Feynman Lectures on Physics Boston, MA, USA," *Section 4-1 (The Conservation of Energy Principle)*, vol. 1, no. 12, pp. pp. 4-2–4-3, 2005.

Corresponding author: Amanya Denis
amanyadenis777@gmail.com
Department of Electrical Engineering, Faculty of Engineering, Technology, Applied Design and Fine Art, Kabale University, Uganda.

[3] R. V. J. B. K. N. A. C. A. G. M. M. T. S. Kim, "Ambient RF energy-harvesting technologies for self-sustainable wireless electronics," *IEEE Microwave Magazine,* vol. 15, no. 6, p. 26–41, November/December 2014.

[4] M. Piñuela, P. D. Mitcheson, S. Lucyszyn, "Ambient RF energy harvesting in urban and semi-urban environments," *IEEE Transactions on Microwave Theory and Techniques,* vol. 61, no. 7, p. 2715–2726, July 2013.

[5] Syed H. Shah, Aqeel A. Khan, James A. Flint, "Metamaterial and Multi-band Antenna Designs for RF Energy Harvesting: A Review," IEEE Access (Open Access Journal), Piscataway, New Jersey, USA, 2016.

[6] Tentzeris, M. M., Georgiadis, A., & Roselli, L., "Energy harvesting and scavenging. Proceedings of the IEEE," New York, NY, USA, 22 February 2017. [Online]. Available: https://doi.org/10.1109/JPROC.2017.2708661. [Accessed 1 December 2025].

[7] A. A. G. Amer, N. Othman, S. Z. Sapuan, A. Alphones, M. F. Hassan, A. J. A. Al-Gburi and Z. Zakaria, Dual-Band, Wide-Angle, and High-Capture Efficiency Metasurface for Electromagnetic Energy Harvesting, Basel, Switzerland: Nanomaterials (Basel: MDPI), 2023.

[8] Z. L. &. W. W. Wang, "Nanotechnology-enabled energy harvesting for self-powered micro-/nanosystems," *Angewandte Chemie International Edition,* vol. 51, no. 47, pp. 11700-11721., 2012.

[9] J. &. Y. S. Choi, Rectification efficiency improvement in RF energy harvesting circuits using adaptive impedance matching. Energy Conversion and Management, Netherlands: Amsterdam, 2017.

[10] Joseph A. Paradiso & Thad Starner, "Energy scavenging for mobile and wireless electronics," *IEEE Pervasive Computing,* vol. 4, no. 1, p. 18–27, 2005.

[11] Ugwuogo, J., "Demand Energy Harvesting Techniques," University of Waterloo, Waterloo, Canada, , 2012.

[12] Qudrat Ullah- IEEE Sensors Journal, "Energy Reports," *The practical applications of RF energy harvesting have expanded significantly, especially in powering low-power devices such as sensors, IoT modules, wearable electronics, and even biomedical implants,* pp. 34-39, 10 January 2025.

[13] K. D. M. Rajesh, "Energy harvesting techniques for self-sustaining wearables in remote environments," New York, 2019.

Corresponding author: Amanya Denis
amanyadenis777@gmail.com
Department of Electrical Engineering, Faculty of Engineering, Technology, Applied Design and Fine Art, Kabale University, Uganda.